INTERNATIONAL JOURNAL FOR NUMERICAL METHODS IN FLUIDS, VOL. 20, 831–851 (1995)

AN *hp* ADAPTIVE STRATEGY FOR FINITE ELEMENT APPROXIMATIONS OF THE NAVIER–STOKES EQUATIONS

J. TINSLEY ODEN, WEIHAN WU

TICAM Office, The University of Texas at Austin, Austin, TX. 78712, U.S.A.

VINCENT LEGAT

CESAME, Universite Catholique de Louvain, B-1348, Louvain-la-Neuve, Belgium

SUMMARY

Recently, a rigorous *a posteriori* error estimate, based on the element residual method, for the steady-state Navier–Stokes equations has been derived. In this paper, by using this error estimate, we construct an *hp* adaptive strategy to minimize the total computation costs while achieving a targeted accuracy for steady incompressible viscous flow problems. The basic *hp* adaptive strategy is to solve the approximate problem in three consecutive stages corresponding to three different meshes, i.e. an initial mesh, an intermediate adaptive *h*-mesh, and a final adaptive *hp* mesh. Our numerical result shows that the three-step *hp* adaptive strategy for the incompressible flow problems indeed provides an accurate approximate solution while keeping the computational costs under control.

KEY WORDS: error estimation; adaptivity; *hp*-methods; Navier–Stokes

1. INTRODUCTION

The goal of *hp* adaptive finite element methods is to obtain an accurate approximate solution within a preset error tolerance at the least possible computational cost, mainly measured in terms of the total CPU time and the total computer memory used. There are two major questions that must be resolved in order to reach this goal. One is how to estimate the accuracy of approximate solutions when exact solutions are not available; the other concerns the control of computational costs to obtain the user-specified error tolerance. The issue of estimating the error of approximate solution for the steady-state Navier–Stokes equations is discussed in[1,2] while the issue of designing an *hp* adaptive strategy[3] is considered here.

To control computational costs, one needs to develop an efficient *hp* adaptive strategy for obtaining near-optimal adaptive *hp* meshes. The payoff can be considerable: exponential rates of convergence with respect to the computed error can be achieved by using very few degrees of freedom, and this translates into meshes which deliver targeted accuracies with many fewer degrees of freedom than traditional *h*- or *p*-version methods. On the other hand, the total computational overhead in an unplanned adaptive *hp* strategy can conceivably be greater than the cost for conventional uniform *h* or *p* methods. To overcome this potential complication, a prudently designed adaptive strategy is required.

The research in the design of efficient adaptive strategies is still in early stages. The first general *hp* adaptive strategy was proposed by Rachowicz *et al.*[4] in 1989, which involved a scheme requiring many steps of solving linear system for different stages of mesh in order to achieve an

CCC 0271–2091/95/080831–21

optimal mesh. Recently Oden *et al.*[3] developed an efficient three-step *hp* adaptive strategy in which employs only three stages corresponding to three different meshes. Initial numerical experiments using the three-step *hp* adaptive strategy are encouraging when the total CPU time needed is compared with those of uniform *h* or *p* methods. The current study extends this *hp* adaptive strategy to the steady-state Navier–Stokes flow problem.

Following this introduction, the Navier–Stokes equations and the basic notations used in this paper will be presented in Section 2. The finite element approximations of the Navier–Stokes equations is described in Section 3. In Section 4, two major theorems on the *a posteriori* error estimation for steady-state Navier–Stokes equations are given. The three-step *hp* adaptive strategy is presented in Section 5. Finally, results of numerical experiments are given in Section 6.

2. THE NAVIER–STOKES EQUATIONS

The steady-state Navier–Stokes equations on a bounded Lipschitz domain $\Omega \in \mathbb{R}^n$, $n = 2$ or 3, are described as follows:

$$\begin{aligned} (\mathbf{u}\cdot\nabla)\mathbf{u} - \nabla\cdot\boldsymbol{\sigma}(\mathbf{u}, p) &= \mathbf{f} \quad \text{in } \Omega \\ \nabla\cdot\mathbf{u} &= 0 \quad \text{in } \Omega \\ \mathbf{u} &= 0 \quad \text{on } \partial\Omega \end{aligned} \tag{1}$$

where $\mathbf{u} = \mathbf{u}(\mathbf{x})$, $\mathbf{x} = (x_1, \ldots, x_n) \in \Omega$, is the velocity field, and $\mathbf{f}$ is the body force. $\boldsymbol{\sigma}(\mathbf{u}, p)$, the Cauchy stress, is defined as $2\nu\mathbf{D}(\mathbf{u}) - p\mathbf{1}$ with the kinematic viscosity $\nu > 0$, strain rate tensor $\mathbf{D}(\mathbf{u}) = (\nabla\mathbf{u} + \nabla\mathbf{u}^{\mathrm{T}})/2$, pressure p, and the unit tensor $\mathbf{1}$.

To obtain a weak formulation of (1), we introduce the following spaces and norms:

$$V = (H_0^{1\,V}(\Omega))^n$$

$$H = \{\mathbf{v} \in V\colon \operatorname{div}\mathbf{v} = 0\}$$

$$|\mathbf{v}|_1^2 = \int_\Omega \nabla\mathbf{v}\colon \nabla\mathbf{v}\,\mathrm{d}x = \int_\Omega \sum_{i,j=1}^{n} \frac{\partial v_i}{\partial x_j}\frac{\partial v_i}{\partial x_j}\,\mathrm{d}x$$

$$Q = \left\{q \in L^2(\Omega)\colon \int_\Omega q\,\mathrm{d}x = 0\right\}$$

$$\|q\|_0^2 = \int_\Omega q^2\,\mathrm{d}x$$

where $\mathrm{d}x = \mathrm{d}x_1\,\mathrm{d}x_2 \ldots \mathrm{d}x_n$ with the trilinear, bilinear, and linear forms,

$$c\colon V \times V \times V \to \mathbb{R}, \quad c(\mathbf{u}, \mathbf{v}, \mathbf{w}) = \int_\Omega \mathbf{u}\cdot\nabla\mathbf{v}\cdot\mathbf{w}\,\mathrm{d}x$$

$$a\colon V \times V \to \mathbb{R}, \quad a(\mathbf{u}, \mathbf{v}) = \int_\Omega 2\nu\mathbf{D}(\mathbf{u})\colon\mathbf{D}(\mathbf{v})\,\mathrm{d}x$$

$$b\colon Q \times V \to \mathbb{R}, \quad b(q, \mathbf{v}) = \int_\Omega q\nabla\cdot\mathbf{v}\,\mathrm{d}x$$

$$f\colon V \to \mathbb{R}, \quad f(\mathbf{v}) = \int_\Omega \mathbf{f}\cdot\mathbf{v}\,\mathrm{d}x$$

Then the weak formulation of Navier–Stokes equations is

$$\boxed{\begin{aligned}&\text{Find } (\mathbf{u}, p)\in V\times Q \text{ such that for all } (\mathbf{v}, q)\in V\times Q,\\ &c(\mathbf{u},\mathbf{u},\mathbf{v}) + a(\mathbf{u},\mathbf{v}) - b(p,\mathbf{v}) = f(\mathbf{v})\\ &b(q,\mathbf{u}) = 0.\end{aligned}} \tag{2}$$

The forms $a(\cdot,\cdot)$, $b(\cdot,\cdot)$, $c(\cdot,\cdot,\cdot)$, and $f(\cdot)$ are continuous and $b(\cdot,\cdot)$ satisfies inf sup condition.[5] Also, we assume that there exists a constant γ such that

$$\gamma = \sup_{\mathbf{u},\mathbf{v},\mathbf{w}\in H} \frac{|c(\mathbf{u},\mathbf{v},\mathbf{w})|}{|\mathbf{u}|_1 |\mathbf{v}|_1 |\mathbf{w}|_1} \tag{3}$$

the data body force $\mathbf{f}$ is defined such that it corresponds to a functional

$$f\in (H^{-1})' \tag{4}$$

with norm being defined as

$$\|f\|^* = \sup_{\mathbf{v}\in H\setminus 0} \frac{|f(\mathbf{v})|}{|\mathbf{v}|_{1,\Omega}} \tag{5}$$

Under these conditions, the existence and uniqueness of solutions of (2) are given as follows.

Theorem 1. (i) *Under the above definitions and conditions, there exists at least one solution* $(\mathbf{u}, p)\in V\times Q$ *to problem* (2).

(ii) *If, in addition,*

$$\|f\|^* < \nu^2/\gamma \tag{6}$$

then the solution $(\mathbf{u}, p)$ *is unique.*

Proof: See Reference 6. □

3. FINITE ELEMENT APPROXIMATIONS

To develop finite element approximations of (2), we introduce a partition $\mathscr{P}$ of Ω into a collection of $N = N(\mathscr{P})$ subdomains Ω_K:

$$\bar{\Omega} = \bigcap_{K=1}^{N(\mathscr{P})} \bar{\Omega}_K,\ \Omega_K\cap\Omega_L = \emptyset \quad \forall K\neq L$$

We may now write

$$a(\mathbf{u},\mathbf{v}) = \sum_{K=1}^{N} a_K(\mathbf{u},\mathbf{v})$$

$$a_K(\mathbf{u},\mathbf{v}) = \int_{\Omega_K} 2\nu \mathbf{D}(\mathbf{u}):\mathbf{D}(\mathbf{v})\,dx, \quad \mathbf{u},\mathbf{v}\in V_K$$

$$b(q,\mathbf{v}) = \sum_{K=1}^{N} b_K(q,\mathbf{v})$$

$$b_K(q,\mathbf{v}) = \int_{\Omega_K} q\nabla\cdot\mathbf{v}\,dx, \quad q\in Q_K, \mathbf{v}\in V_K$$

etc., with similar definitions for $c_K(\cdot,\cdot,\cdot)$, $f_K(\cdot)$, where $V_K = V(\Omega_K)$ and $Q_K = \{q \in L^2(K): q = p|_K, p \in Q\}$ denote corresponding local spaces of functions in V and Q, respectively, restricted to Ω_K.

Following the standard finite element approaches, let Ω and $\mathscr{P}$ be constructed such that each subdomain Ω_K is the image of a master element $\hat{\Omega}$ under an affine invertible map $F_K: \hat{\Omega} \to \Omega_K$, $1 \leqslant K \leqslant N$. If $\xi = F_K^{-1}(\mathbf{x})$, $\mathbf{x} \in \bar{\Omega}_K$, we approximate test functions $\mathbf{v} \in V_K$, $q \in Q_K$ by functions $\mathbf{v}^h$ and q^h such that $\hat{v}_i(\xi) = v_i^h \circ F_K^{-1}(\mathbf{x})$, $1 \leqslant i \leqslant n$, $\hat{q}(\xi) = q^h \circ F_K^{-1}(\mathbf{x})$ are polynomials or products of polynomials in ξ. The resulting spaces of functions have the properties $V_K^h \subset V_K$ and $Q_K^h \subset Q_K$.

The finite element approximation of (2) obtained using the spaces V^h and Q^h is characterized by the following discrete problem.

$$\boxed{\begin{aligned}&\text{Find } (\mathbf{u}^h, p^h) \in V^h \times Q^h \text{ such that for every } (\mathbf{v}^h, q^h) \in V^h \times Q^h,\\ &\qquad c(\mathbf{u}^h, \mathbf{u}^h, \mathbf{v}^h) + a(\mathbf{u}^h, \mathbf{v}^h) - b(p^h, \mathbf{v}^h) = f(\mathbf{v}^h),\\ &\qquad\qquad b(q^h, \mathbf{u}^h) = 0.\end{aligned}} \tag{7}$$

Under proper conditions, one can construct convergent sequences of solutions to (7). See Reference 6 for details. Moreover, the following result can be established.

Theorem 2. Let $n \leqslant 3$ and the conditions of Theorem 1 hold. Let $(\mathbf{u}, p)$ be the solution of (1). Then, for ν sufficiently large, there exists an h_0 such that for all $h \leqslant h_0$, (7) has a unique solution $(\mathbf{u}^h, p^h) \in V^h \times Q^h$ and

$$\lim_{h \to 0} \{|\mathbf{u} - \mathbf{u}^h|_1 + \|p - p^h\|_0\} = 0 \tag{8}$$

If, in addition, the solution $(\mathbf{u}, p)$ of $(3) \in (H^{k+1}(\Omega)^n \cap V) \times (H^k(\Omega) \cap Q)$ for $k \leqslant \ell$, then a constant $C > 0$ exists, independent of h, such that

$$|\mathbf{u} - \mathbf{u}^h|_1 + \|p - p^h\|_0 \leqslant Ch^k \tag{9}$$

Proof. See Reference 6, in particular pp. 317–318. □

4. THE *A POSTERIORI* ERROR ESTIMATE FOR THE STEADY-STATE NAVIER–STOKES EQUATIONS

Now we shall construct an *a posteriori* error estimate for the Navier–Stokes equations. Let $(\mathbf{u}, p)$ and $(\mathbf{u}^h, p^h)$ be the unique solutions to the problems (1) and (7), respectively.

Define two bilinear forms as

$$\begin{aligned}A(\mathbf{u}, \mathbf{v}) &= \int_\Omega 2\nu \mathbf{D}(\mathbf{u}) : \mathbf{D}(\mathbf{v})\, dx\\ B(p, q) &= \int_\Omega p \cdot q\, dx\end{aligned} \tag{10}$$

and the pair $(\varphi, \psi) \in V \times Q$ which are solutions of

$$\begin{aligned}A(\varphi, \mathbf{v}) &= a(\mathbf{e}, \mathbf{v}) - b(E, \mathbf{v}) + c(\mathbf{u}, \mathbf{u}, \mathbf{v}) - c(\mathbf{u}^h, \mathbf{u}^h, \mathbf{v})\\ B(\psi, q) &= -b(q, \mathbf{e}) \quad \forall (\mathbf{v}, q) \in V \times Q\end{aligned} \tag{11}$$

where $\mathbf{e} = \mathbf{u} - \mathbf{u}^h$ and $E = p - p^h$.

The existence and uniqueness of the pair (φ, ψ) in (11) follows immediately from the definitions of A and B in (10). Next we define the 'star norm' of error to be

$$\|(\mathbf{e}, E)\|_*^2 = |\varphi|_A^2 + |\psi|_0^2 \tag{12}$$

with

$$\begin{aligned} |\varphi|_A^2 &= A(\varphi, \varphi) \\ |\psi|_0^2 &= B(\psi, \psi) \end{aligned} \tag{13}$$

The 'averaged' approximate flux on the boundary Γ_{KL} is defined as

$$\langle \mathbf{n}_K \cdot \boldsymbol{\sigma}(\mathbf{u}^h, p^h) \rangle = \mathbf{n}_K \cdot [(1 - \alpha_{KL}(\mathbf{s}))\boldsymbol{\sigma}_K(\mathbf{u}^h, p^h) + \alpha_{KL}(\mathbf{s})\boldsymbol{\sigma}_L(\mathbf{u}^h, p^h)] \tag{14}$$

$\boldsymbol{\sigma}_K$ is the Cauchy stress in $\bar{\Omega}_K$ at $\mathbf{s} \in \Gamma_{KL}$ and $\boldsymbol{\sigma}_L$ is that in neighboring element $\bar{\Omega}_L$ at $\mathbf{s}$. Thus, (14) defines a linear combination of approximate boundary fluxes on the interelement boundary. Note that if we take $\alpha_{KL} = \frac{1}{2}$, (14) reduces to a simple average of fluxes. We shall assume hereafter that the parameter functions α_{KL} are constructed in such a way that the element residual and boundary residuals are balanced in the sense of References 7, 8, i.e. the residual fluxes are *equilibrated.*

The following theorem confirms that the star norm defined in (12) is actually equivalent to the usual norm used for the Navier–Stokes equation.

Theorem 3. Let the conditions of Theorems 1 *and* 2 *hold for* $k > 0$ *and, moreover, there exists a constant* L *such that*

$$|\mathbf{u}|_1 \leqslant L < \nu/\gamma \tag{15}$$

Then there exists two positive constants k_1 *and* k_2 *such that as* $h \to 0$,

$$k_1 \|(\mathbf{e}, E)\|_*^2 \leqslant |\mathbf{e}|_1^2 + \|E\|_0^2 \leqslant k_2 \|(\mathbf{e}, E)\|_*^2 \tag{16}$$

where k_1 *and* k_2 *are positive constants.*

Proof: See References 1 and 2. □

The *a posteriori* error estimate for the Navier–Stokes equations is as follows.

Theorem 4. Let assumptions on Theorem 4 *hold and* $A_K(\cdot, \cdot)$ *and* $B_K(\cdot, \cdot)$ *denote the element inner products corresponding to* $A(\cdot, \cdot)$ *and* $B(\cdot, \cdot)$ *of* (10) *and let* $\varphi_K \in V_K$ *denote the solution of the local error residual problem,*

$$A_K(\varphi_K, \mathbf{v}_K) = f_K(\mathbf{v}_K) - a_K(\mathbf{u}_K^h, \mathbf{v}_K) + b_K(p_K^h, \mathbf{v}_K) - c_K(\mathbf{u}_K^h, \mathbf{u}_K^h, \mathbf{v}_K) + \oint_{\partial\Omega_K/\partial\Omega} \langle \mathbf{n}_K \cdot \boldsymbol{\sigma}(\mathbf{u}^h, p^h) \rangle \cdot \mathbf{v}_K \, ds \tag{17}$$

for every $\mathbf{v}_K \in V_K$, $1 \leqslant K \leqslant N$. *Then the error* $(\mathbf{e}, E)$ *of the finite element approximations of the Navier–Stokes equations* (1) *satisfies the following bound*:

$$\|(\mathbf{e}, E)\|_*^2 \leqslant \sum_{K=1}^{N} \|(\varphi_K, \operatorname{div} \mathbf{u}_K^h)\|_{*,K}^2 \tag{18}$$

Proof. See Reference 1. □

5. THE THREE-STEP h–p ADAPTIVE STRATEGY

Here, we employ the three-step scheme introduced in Reference 3 and exploited in Reference 9 and elsewhere. For completeness, we record its basic properties. The goal of the three-step adaptive strategy is to reach a preset target error of the problem and to minimize the computational effort required.

To develop the scheme, we suppose that a global *a priori* error estimate exists in the star norm[10]

$$\|(\mathbf{e}, E)\|_*^2 \leqslant \sum_{K=1}^{N(\mathscr{P})} \frac{h_K^{2\mu_K}}{p_K^{2\nu_K}} \Lambda_K^2 \tag{19}$$

where h_K, p_K are, respectively, the size and the spectral order of the element K, ν_K and μ_K depend on the regularity of solutions and Λ_K is a local unknown constant. We also define local error indicator θ_K, global error indicator θ and error index η as

$$\theta_K = \|(\varphi_K, \operatorname{div} \mathbf{u}_K^h)\|_{*,K}, \quad \theta = \sqrt{\sum_{K=1}^{N} (\theta_K)^2}, \quad \eta = \frac{\|(\mathbf{e}, E)\|_*}{\|(\mathbf{u}, p)\|_*} \tag{20}$$

Now, we introduce several major assumptions. The asymptotic estimate on (19) is treated as an equality and the actual error is approximated by the *a posteriori* error estimate θ. By setting, respectively, the unknown exponents μ_K and ν_K to given μ, ν, and then passing to the element level, we have the following relation:

$$\theta_K \approx \frac{h_K^{\mu}}{p_K^{\nu}} \Lambda_K \tag{21}$$

Now, we assign a target error index η^{tgt} and we are able to describe the three steps as follows:

(a) Introduce an initial mesh $\mathscr{P}^0$ with a sufficient number N^0 elements such that the approximate solution will fall into the asymptotic part of the convergence curve. Solve the problem on this mesh and calculate the local *a posteriori* error indicator θ_K^0 on $\mathscr{P}^0$ to estimate the error. We then estimate the star norm of the exact solution and the initial error index by

$$\|(\mathbf{u}, p)\|_*^2 \approx \|(\mathbf{u}^0, p^0)\|_*^2 \approx \|(\mathbf{u}^{h0}, p^{h0})\|_*^2 + (\theta^0)^2$$

$$\eta^0 \approx \frac{\theta^0}{\|(\mathbf{u}^0, p^0)\|_*}$$

Select η^{int} such that $\eta^{\text{tgt}} \leqslant \eta^{\text{int}} \leqslant \eta^0$.

(b) Calculate the number n_K of new subelements required in each element of $\mathscr{P}^0$ in order to obtain a new optimal mesh $\mathscr{P}^1$ with N^1 elements while achieving the required intermediate error index η^{int}.

Considering an uniform h-refinements on element K of $\mathscr{P}^0$, the number of subelements on element K can be correlated by $n_K = (h_K^0/h_K^1)^{2/\beta}$ with $\beta = 2/n$ and n is the dimension of the problem. Using (21), we can easily find the following non-linear system which allows us to compute n_K:

$$n_K = \left[N^1 \frac{(\theta_K^0)^2}{(\theta^{\text{int}})^2} \right]^{1/(\beta_\mu + 1)}$$

$$\sum_{K=1}^{N^0} n_K = N^1 \tag{22}$$

where the global error θ^{int} is predicted by $\eta^{\text{int}} \|(\mathbf{u}^0, p^0)\|_*$. Having n_K, we introduce h-refinements on $\mathscr{P}^0$ to construct $\mathscr{P}^1$.

Now, solve the problem on this second mesh and compute the local *a posteriori* error indicators θ_K^1.

(c) The third mesh $\mathscr{P}^2$ is constructed by calculating a distribution of polynomial degrees p_K of $\mathscr{P}^1$ to reach the target error index η^{tgt}. From (21), we can calculate the required spectral order p_K of $\mathscr{P}^1$ to obtain an equally distributed target error on the new mesh by

$$p_K = \left[\sqrt{N^1} \frac{(\theta_K^1)(p_K^0)^\nu}{(\theta^{\text{tgt}})} \right]^{1/\nu} \tag{23}$$

where the global error θ^{tgt} is predicted by $\eta^{\text{tgt}} \|(\mathbf{u}^1, p^1)\|_*$.

Now, enrich p on each element of $\mathscr{P}^1$ to obtain $\mathscr{P}^2$. Solve the problem on $\mathscr{P}^2$ and compute the final error index η^2. If $\eta^2 \leqslant \eta^{\text{tgt}}$, the computation is terminated; otherwise the whole procedure is repeated.

This technique provides a good compromise between the cost of the adaptivity and the quality of the final mesh. In fact, it leads to good (but suboptimal) meshes and exhibits fast convergence characteristics with respect to CPU time from our numerical examples.

6. NUMERICAL RESULTS

In the following three examples, the initial mesh is selected according to the physical geometry of flow problem. The flow is solved by using usual Newton–Raphson iterative solver with continuous velocity and pressure on elements with spectral order as $Q2/Q1$ (i.e. biquadratic velocity and bilinear pressure), $Q3/Q2$, $Q4/3$, $Qp/Q(p-2)$ for $p \geqslant 5$. A continuation method is used to reach steady-state solution for the initial mesh with initial guess came from the computed solution of corresponding Stokes problem; however, for the intermediate and final step, the computed solution from the previous mesh is used as an initial guess for the Newton–Raphson solver. For each Newton's step, a direct frontal solver is used.

6.1. *Flow over the cavity* ($Re = 400$)

We consider the problem of the internal flow over the cavity. The Reynolds number is set to be 400 with characteristic length and velocity based on the inflow channel width and averaged

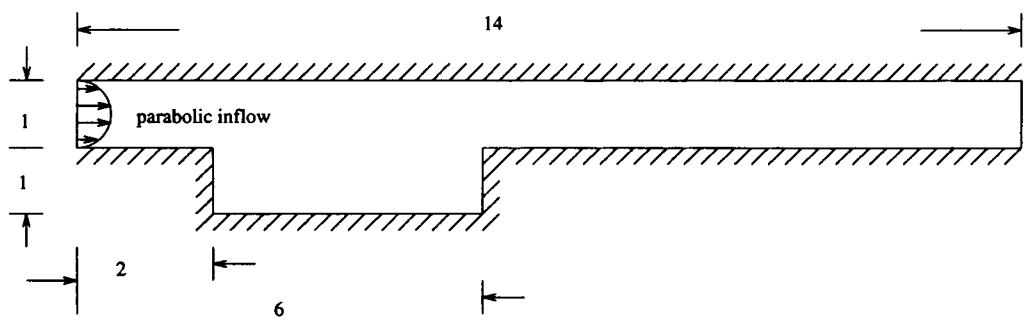

Figure 1. Geometry of flow over cavity with $Re = 400$

inflow velocity. A parabolic inflow and an uniform outflow boundary conditions are used. A detailed geometric description is shown in Figure 1. The initial mesh, shown in Figure 2(a), is selected, which features some local h and p refinement near the corner to resolve better the singularity there.

The initial mesh has 527 d.o.f.s per component. By setting the intermediate error criterion η_I and final error criterion η_T to be 10 and 3 per cent of the total energy, we obtain the

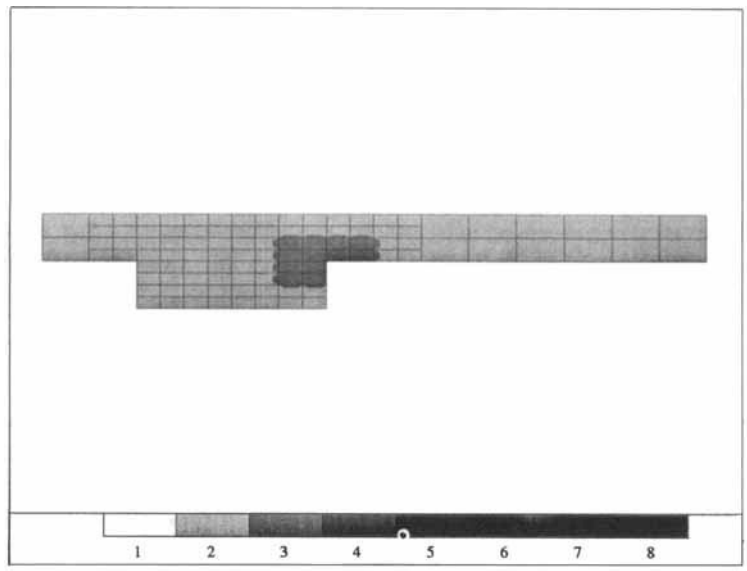

(a)

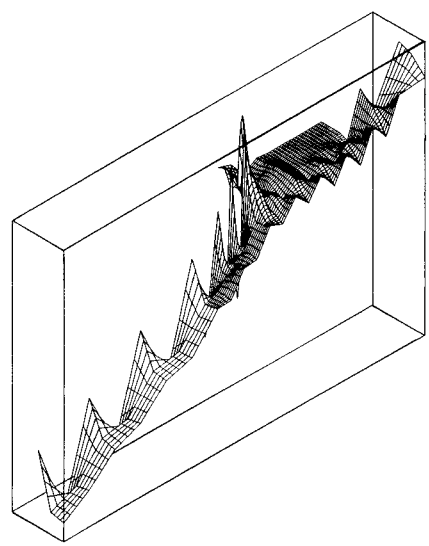

(b)

Figure 2. (a, b)

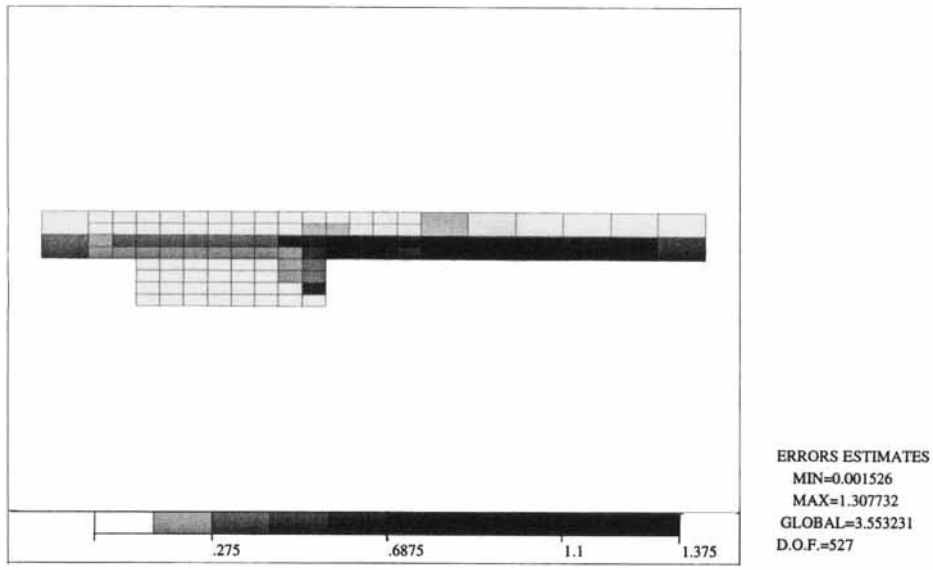

Figure 2. The initial step: (a) initial mesh; (b) computed pressure; (c) error distribution

intermediate mesh and final mesh, as shown in Figures 3(a) and 4(a), with degrees of freedom of 1580 and 1835, respectively. We observe that, in the initial mesh in regions of high error the pressure exhibits severe oscillations, (Figures 2(b) and 2(c)) suggesting that the error is dominated by a poor satisfaction of the incompressibility condition in these regions. After a first adaptive

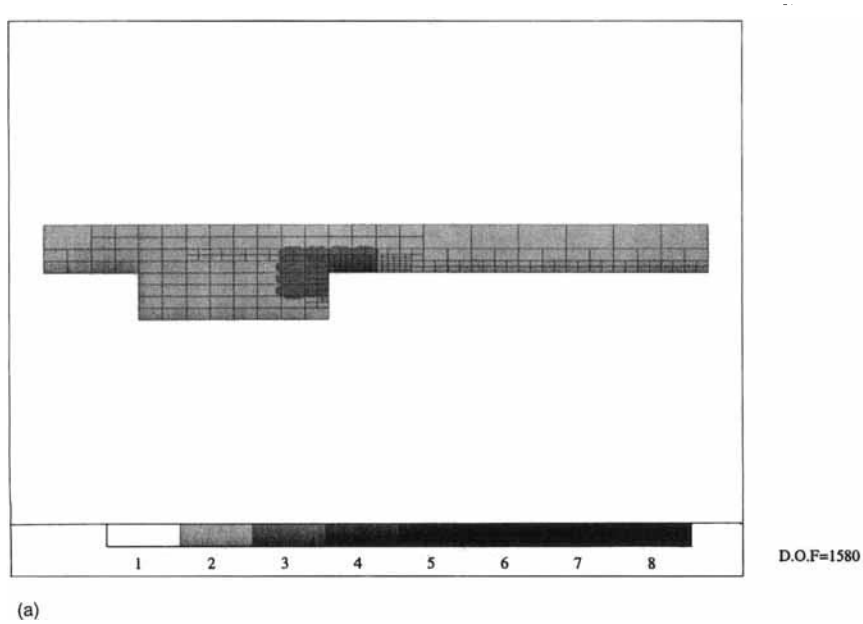

Figure 3. (a)

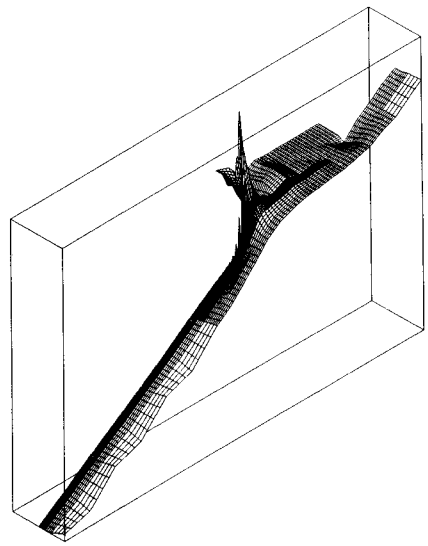

MIN=-.579E-04
MAX=.4703712

(b)

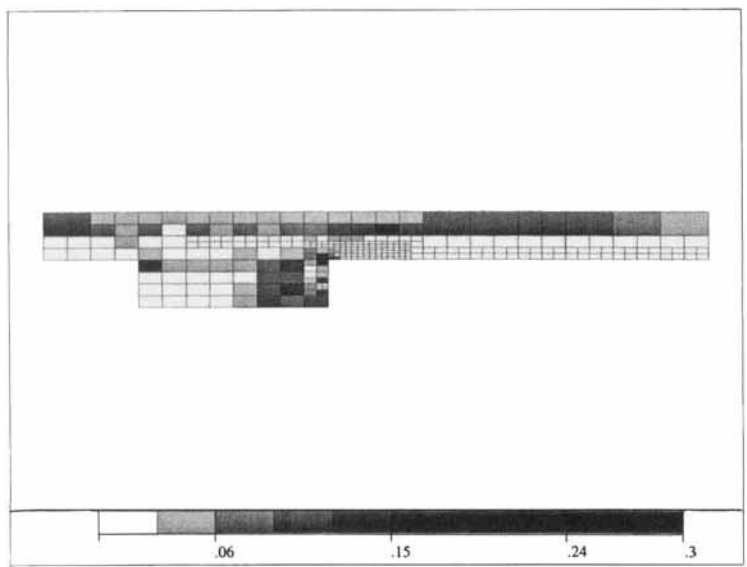

ERRORS ESTIMATES
MIN=0.144E-03
MAX=0.284291
GLOBAL=.794285
D.O.F.=1580

(c)

Figure 3. The intermediate step: (a) intermediate mesh; (b) computed pressure; (c) error distribution

h-refinement, the oscillation observed from the pressure, Figures 2(b) and 3(b), is under control. The second adaptive p-refinement is applied to obtain an approximate solution with an accuracy within the target error. We note that it is not necessary to compute the error for each element for each step. In practice, one can avoid recalculating the error for the elements with very small

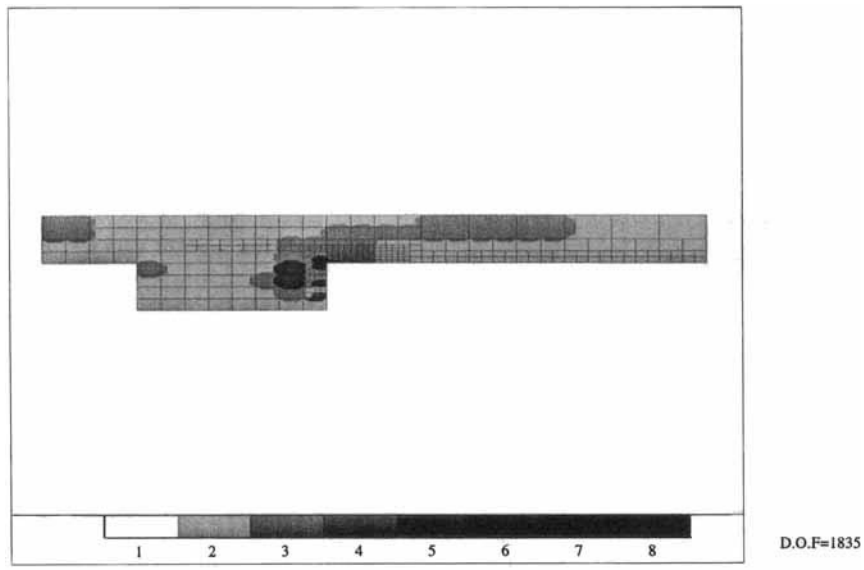

(a)

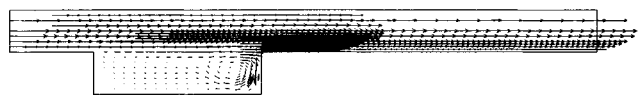

(b)

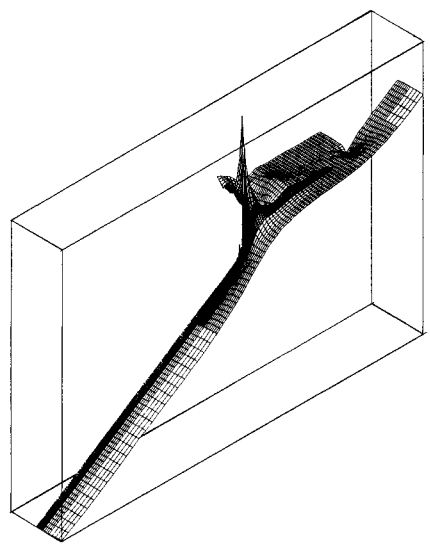

(c)

Figure 4. (a–c)

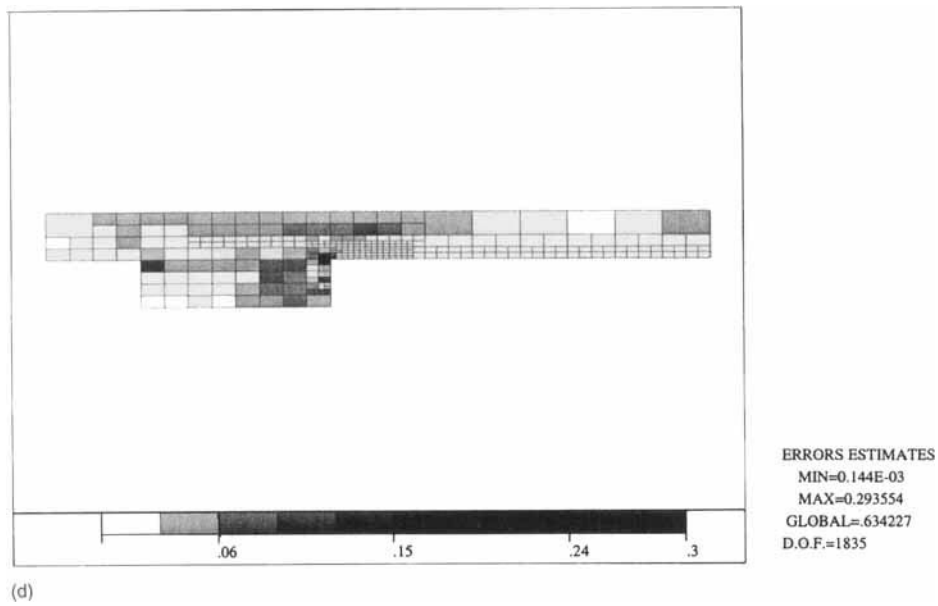

Figure 4. The final step: (a) final mesh; (b) computed velocity vector; (c) computed pressure; (d) error distribution

estimated error after the first step and assume that the error at the later steps is the same as the first step. The final velocity vector picture is shown as Figure 4(b). The final pressure, as shown in Figure 4(c), provides a good approximation when compared with a separate approximate solution obtained by solving the problem on a much finer mesh.

6.2. *Flow over the obstacle* ($Re = 200$)

Next we consider the flow over an obstacle, as shown in Figure 5, with a Reynolds number of 200 based on the inflow channel length and averaged inflow velocity. The initial mesh contains uniform $Q3/Q2$ elements, as shown in Figure 6(a). The computed solutions shown in Figures 6(b) and 6(c) from the initial mesh are highly oscillatory, which indicates that the initial mesh is too coarse to resolve sufficiently the complicated flow characteristics. Conventionally, for this type of convection–diffusion problem, there are mainly two approaches to suppress oscillatory phenomena. One popular approach is to use upwind schemes, e.g. SUPG (streamline upwind

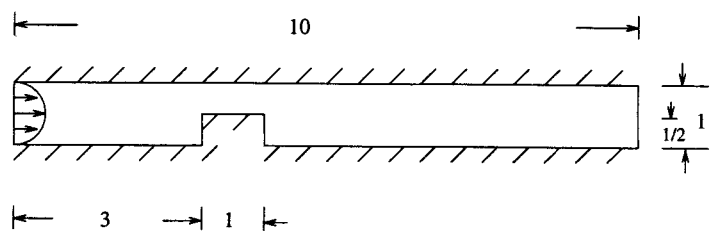

Figure 5. Geometry of flow over the obstacle with $Re = 200$

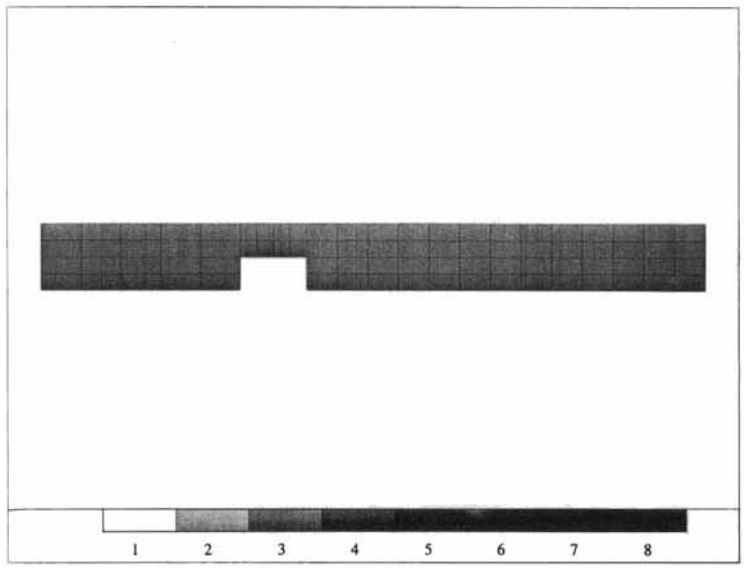

(a)

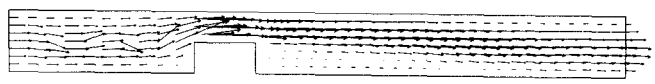

(b)

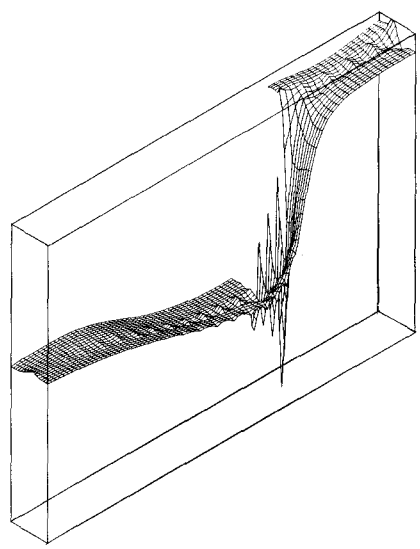

(c)

Figure 6. (a–c)

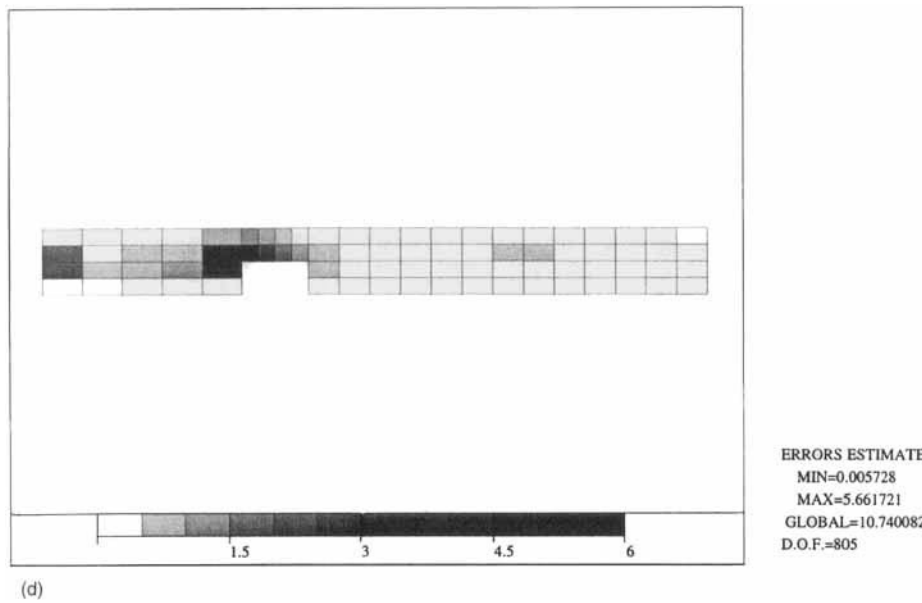

Figure 6. The initial step: (a) initial mesh; (b) computed velocity vector; (c) computed pressure; (d) error distribution

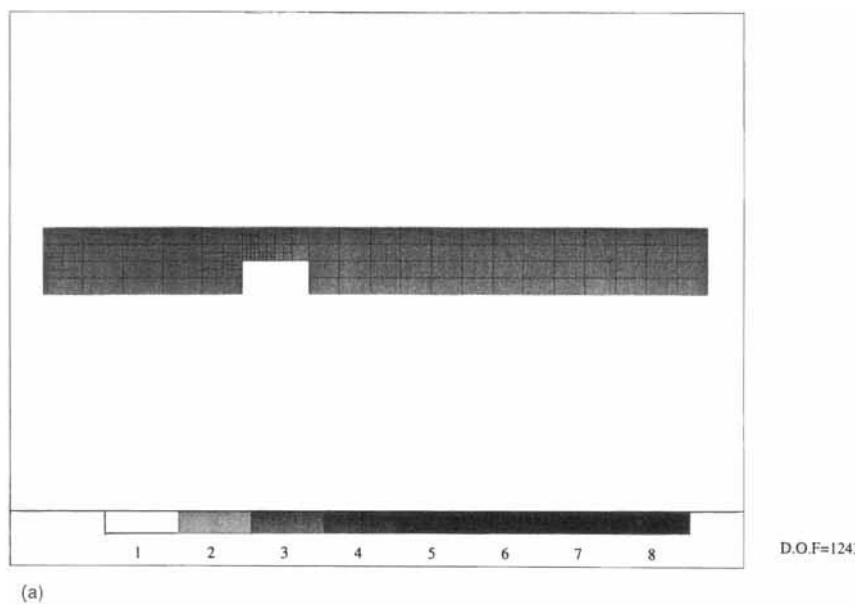

Figure 7. (a)

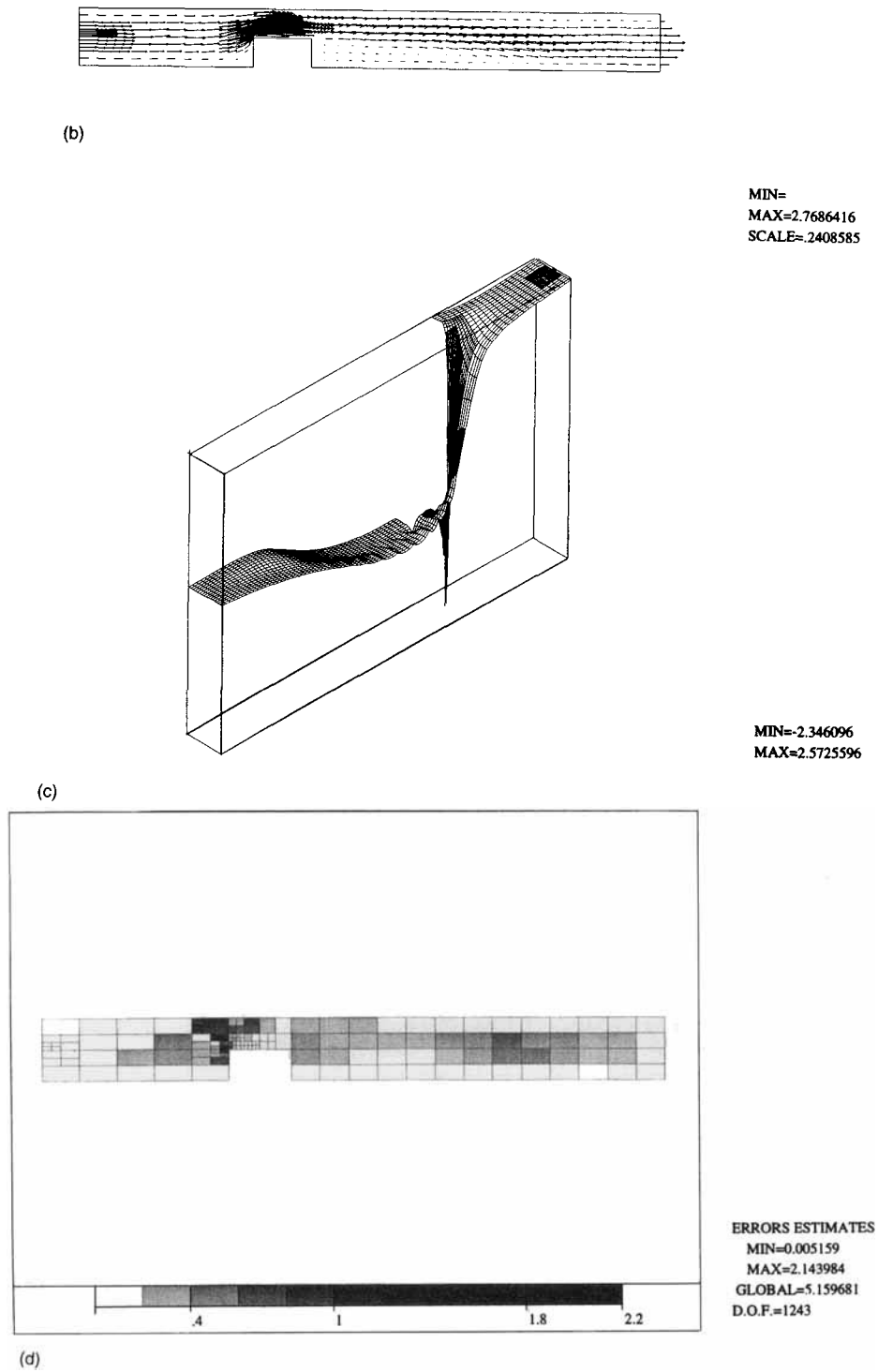

Figure 7. The intermediate step: (a) intermediate mesh; (b) computed velocity vector; (c) computed pressure; (d) error distribution

Petrov–Galerkin methods), which involve modifying the space of test functions so that the flow on the upstream part of elements are assigned more weight than the downstream part. The other approach is simply to refine/enrich the mesh by putting more degrees of freedom on the finite element mesh. Here, the adaptive strategy allows us to refine/enrich the mesh appropriately and obtain an acceptable solution; moreover, the adaptive process stops only if the user-specified

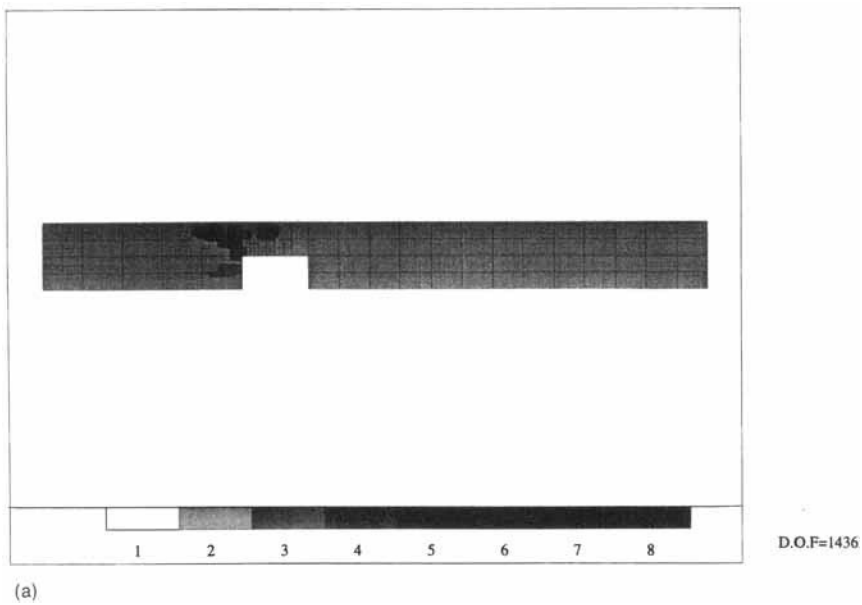

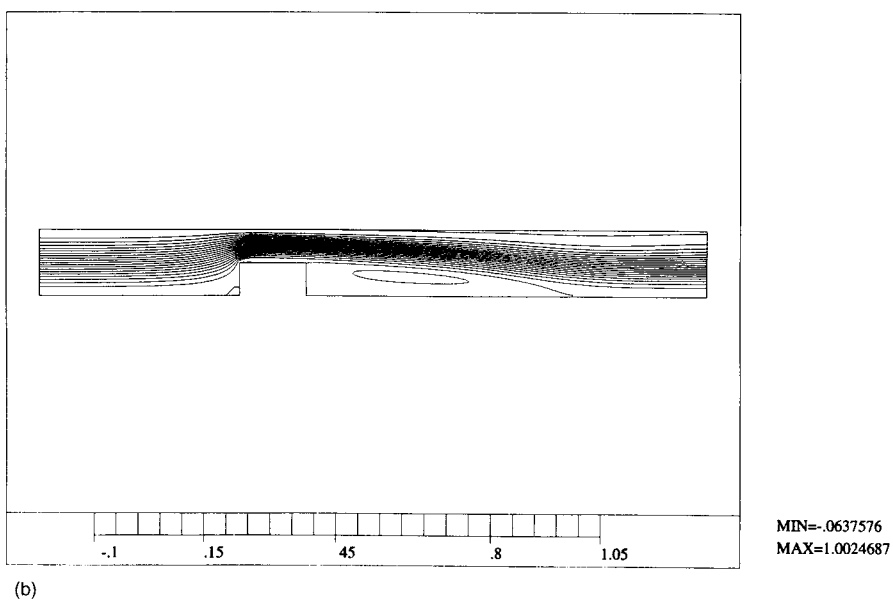

Figure 8. (a, b)

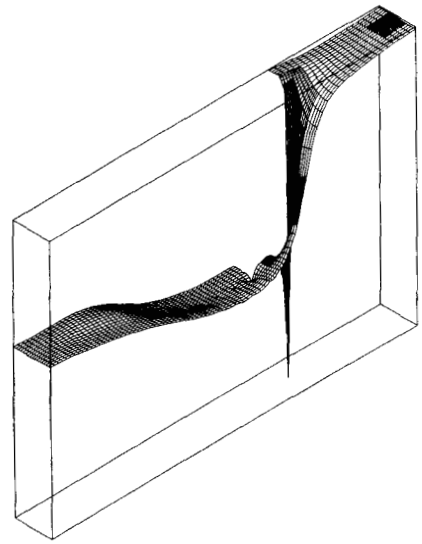

MIN=-2.775708
MAX=2.6714406

(c)

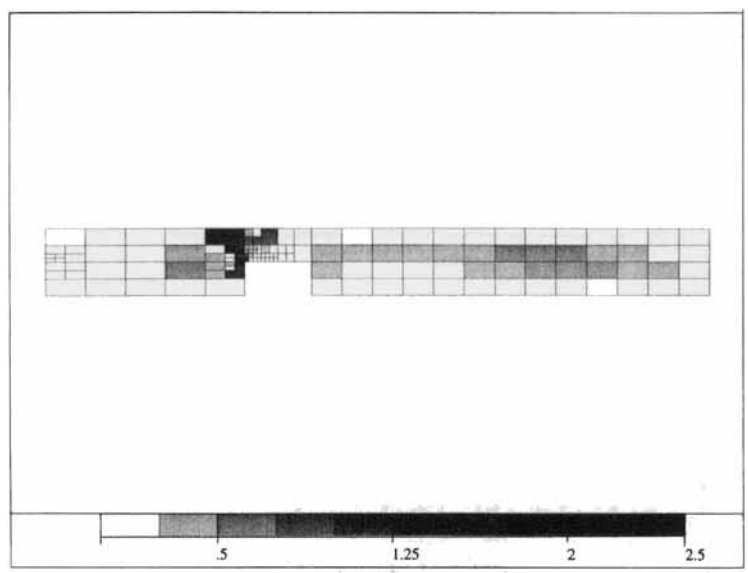

ERRORS ESTIMATES
MIN=0.004771
MAX=2.345653
GLOBAL=5.552734
D.O.F.=1436

(d)

Figure 8. The final step: (a) final mesh; (b) computed streamline; (c) computed pressure; (d) error distribution

error criterion is reached. Following the same adaptive procedure as described previously, we obtain the intermediate mesh and its corresponding solutions and estimated error as shown in Figure 7. The final solution obtained from the h–p adaptive mesh, is shown in Figure 8; the error criterion is met and very little oscillation is observed.

6.3. Backstep channel problems ($Re = 400$)

We consider the steady motion of an isothermal incompressible Newtonian fluid. We impose no-slip conditions on the walls and a fully developed profile in the entry section. The lengths of both channels are, respectively, 2 and 16 lengths of the outflow section. In order to compare our results with Reference 11, we select an inflow section equal to 0·51485 and a Reynolds number of 300. The Reynolds number is based on the average inflow velocity and diameter. The geometry features of the problem are defined in Figure 9.

From an initial mesh of 877 scalar degrees of freedom and a quadratic interpolation, we calculate an estimated error index of 0·14. Then, the three-step strategy is used with an intermediate error index $\eta^{int} = 0{\cdot}10$ and a target error index of $\eta^{tgt} = 0{\cdot}08$. The final mesh is shown in Figure 10. Computed pressure is shown in Figure 11. Close-up views of the three meshes and the error index evolution are shown in Figures 12 and 13. It is expected that the elements are h-refined near the singularity and that orders of $p = 4$ and $p = 3$ are assigned near this point. However, the adaptive strategy also leads to refinements and enrichments in other areas.

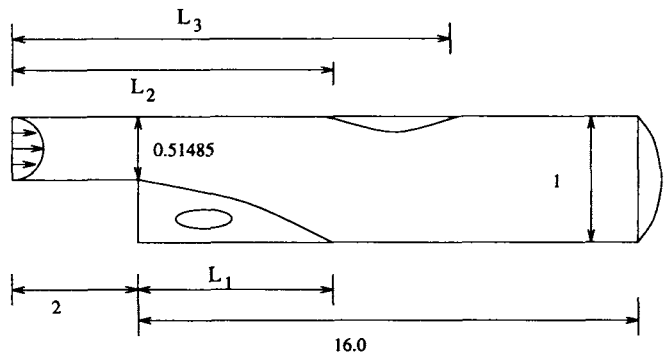

Figure 9. Geometry for the backstep problem

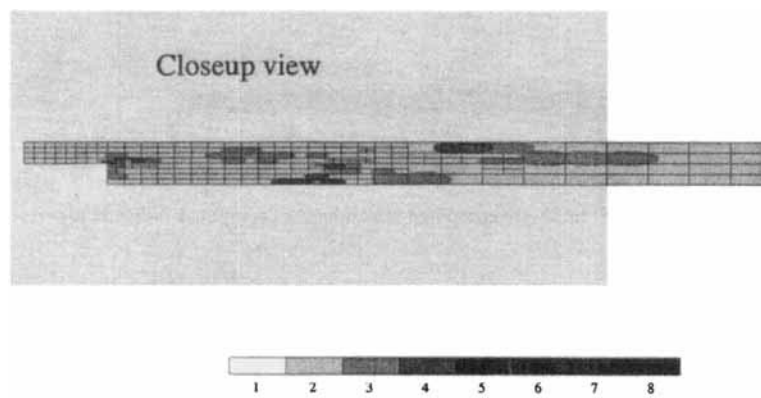

Figure 10. Backstep channel problem ($Re = 300$), Newtonian fluid. Shaded elements reflect non-uniform p-distribution in final mesh

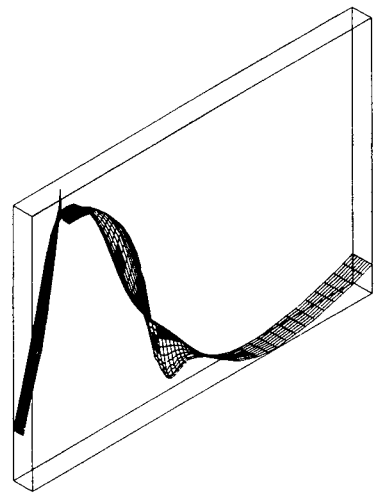

Figure 11. Backstep channel problem (Re = 300), Newtonian fluid. 3-D plot of the pressure

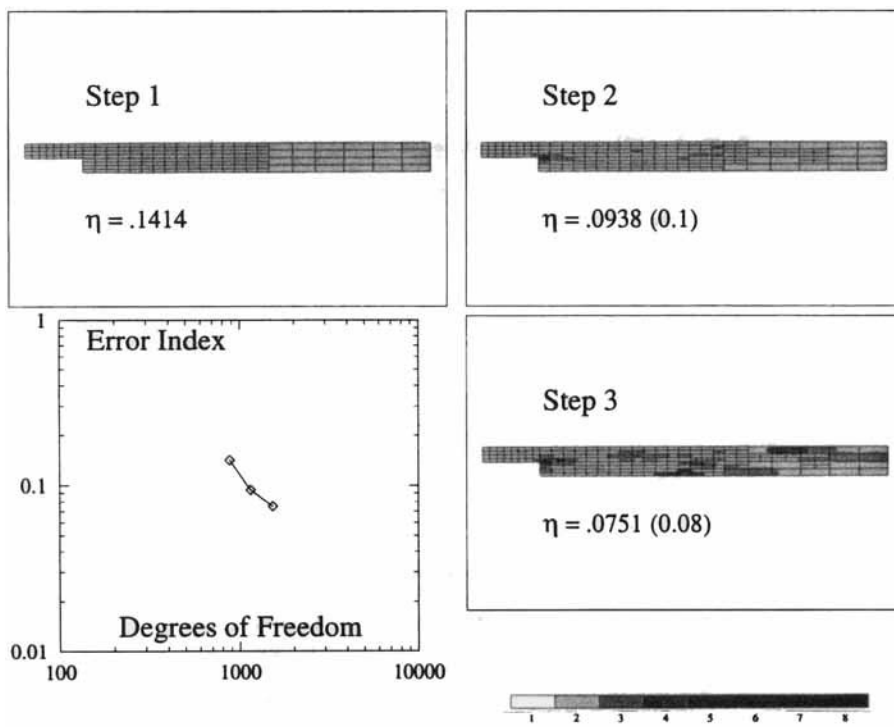

Figure 12. Backstep channel problem (Re = 300), Newtonian fluid. Close-up views of the 3 adaptive meshes

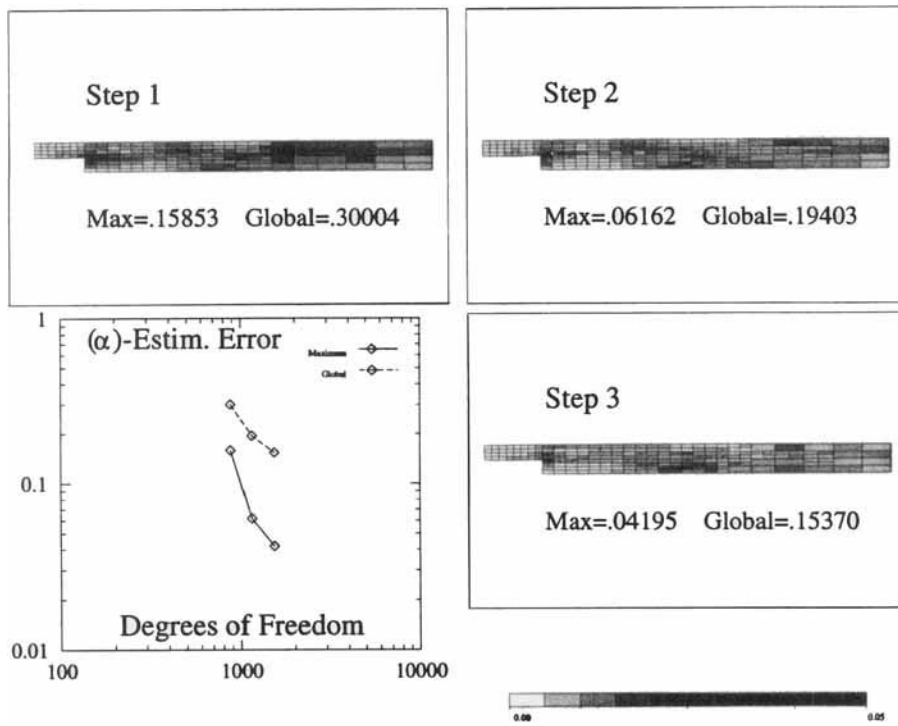

Figure 13. Backstep channel problem ($Re = 300$), Newtonian fluid. Equilibrated estimated error

Table I. CPU time accounting for the backstep problem

Mesh	CPU for the solution (no. of iterations)	CPU for the error estimates	
		(α)	(0·5)
$\mathscr{P}^0$	12246 (21)	1283	866
$\mathscr{P}^1$	3333 (4)	2073	1171
$\mathscr{P}^2$	9264 (5)	3845	2787
Total	24843	7201	4824
	100%	28%	19%

Table II. Backstep problem: reattachement lengths

Reattachement lengths	Reference results[11]	Present results
L_1	4·96	4·95
L_2	4·05	4·13
L_3	7·55	7·32

In order to illustrate the cost of the adaptive strategy, Table I contains the CPU time used for each part of the calculation. The total number of iterations to reach the solution on each mesh (relative variation 10^{-9}) is also provided. Table II contains results seen to be in excellent agreement with the literature. With 1530 scalar degrees of freedoms, values for the reattachement lengths are obtained which agree with those calculated with 12870 d.o.f.'s in Reference 11.

ACKNOWLEDGEMENT

The support of this work by DARPA under Contract #DABT63-92-0042 and of NSF under Grant #ASC9111540 is gratefully acknowledged. One of the authors, V. Legat, wishes to acknowledge the support from the Fonds National de la Recherche Scientifique (FNRS) and from a NATO Research Fellowship.

REFERENCES

1. J. T. Oden, W. Wu and M. Ainsworth, 'An *a posteriori* error estimate for finite element approximations of the Navier–Stokes equations', *Comput. Methods Appl. Mech. Eng.*, **14,** 23–54 (1994).
2. W. Wu, '*h–p* adaptive methods for incompressible viscous flow problems', Ph.D. Dissertation, The University of Texas, Austin, Texas, 1993.
3. J. T. Oden, A. Patra and Y. Feng, 'An *hp* adaptive strategy', in A. K. Noor (ed.), *Adaptive, Multilevel and Hierarchical Computational Strategies*, AMD-Vol 157, ASME, New York, 1992, pp. 23–46.
4. W. Rachowicz, J. T. Oden and L. Demkowicz, 'Toward a universal *h–p* adaptive finite element strategy: Part 3. A study of the design of *h–p* meshes', *Comput. Methods Appl. Mech. Eng.* **77,** 181–212 (1989).
5. R. Temam, *Navier–Stokes Equations: Theory and Numerical Analysis*, Second Printing, North-Holland, Amsterdam, 1985.
6. V. Girault and P.-A. Raviart, *Finite Element Methods for Navier–Stokes Equations*, Springer, Berlin, 1986.
7. M. Ainsworth, and J. T. Oden, 'A unified approach to *a posteriori* error estimation using element residual methods', *Numer. Math.*, **54** (1993).
8. M. Ainsworth and J. T. Oden, 'A procedure for *a posteriori* error estimation for *h–p* finite element methods', *Comput. Methods Appl. Mech. Eng.*, **101,** 73–96 (1992).
9. V. Legat and J. T. Oden, 'An adaptive *hp* finite element method for incompressible free surface flows of generalized newtonian fluids', *ZAMP*, to appear
10. I. Bubujška and M. Suri, 'The *p*- and *h–p* versions of the finite element method: an overview', *Comput. Methods Appl. Mech. Eng.*, **80,** 5–26 (1990).
11. K. N. Ghia, G. A. Osswald and U. Ghai, 'Analysis of incompressible massively separated viscous flows using unsteady Navier–Stokes equations', *Int. j. numer. methods fluids*, **9,** 1025–1050 (1989).